Proceedings of the 4th Pacific Rim Conference on Rheology, August 7~11, Shanghai, China

Bubble Rise Phenomena Through Newtonian and Non-Newtonian Fluids

M.A. Kabir[1], A. R. Slater[1], M.M.K. Khan[1,a] and D. Rackemann[2,b]

[1] *James Goldston Faculty of Engineering and Physical Systems*

Central Queensland University, Rockhampton, QLD-4702, Australia, [a]Email:m.khan@cqu.edu.au

[2] *Sugar Research Institute, Mackay, Qld-4740, Australia, [b]Email:d.rackemann@sri.org.au*

Keywords: Vacuum pan, massecuite, cylindrical column, bubble velocity, bubble trajectory, polymeric solutions.

Abstract. The characteristics of bubble rise phenomenon in three liquids were investigated and are reported here. The experimental rig consists of two transparent cylindrical columns – one a polycarbonate tube of 125 mm diameter and the other an acrylic tube of 400 mm diameter. The rig also consists of a lifting device designed to hold a video camera for taking bubble images. Water and two non-Newtonian fluids (0.025% and 0.045% by weight of polyacrylamide solutions) were used in this study. The smaller polycarbonate tube was used to study the velocity and the drag coefficient under vacuum. The bigger acrylic tube was used to study the influence of the size of bubbles.

Introduction

Steam bubbles play an important role in vacuum pans in sugar industry. The vacuum pan is a large cylindrical steel vessel in which a solution of sugar and water is heated by steam bubbles under vacuum. Bubbles produce very strong circulation inside and above the tubes for mixing of the ingredients in the pan and to create homogeneous conditions for sugar crystallization. Sugar crystals which grow within the solution are removed from the remnant solution and passed on to the next refinement process.

Despite its important applications in sugar industries, a limited research has been carried out on the bubble rise phenomena in massecuite (mixture of crystal and syrup solution). Works by various researchers [1, 3, 4, 5] in general dealt with either bubble movement or heat transfer in bubbles in Newtonian liquids. Massecuite exhibits a non-Newtonian Power-law behaviour and it has a poor optical transparency. Polymeric solutions showing good optical transparency and similar rheological properties to that of massecuite, were used for the investigation of the bubble rise phenomena.

This research investigates bubbles as they rise through a liquid column. The parameters, namely, the bubble velocity, the bubble trajectory and the bubble volume were investigated. The trajectory, the drag coefficient and the velocity were examined for water and 0.025% polyacrylamide solution in the polycarbonate tube whereas the effect of bubble volume was investigated for 0.045% polyacrylamide solution in the acrylic tube. The 0.045% solution had the rheological characteristics similar to that of massecuite. The experimental procedure and the test results of this investigation are presented below.

Experiment

Experimental rig and procedure. The experiments were carried out in two different cylindrical columns and the images of the bubbles for each test were captured by a video camera.

Experimental rig consists of a polycarbonate cylindrical tube (column) of 125 mm diameter and 1.8 m height and an acrylic tube (column) of 250 mm diameter and 1.8 m height. The cylindrical column was manufactured with an aperture at the bottom to allow interchangeable bubble insertion mechanism to be screwed in and used. The bubble insertion mechanism consists of a ladle (an upside–down spoon) attached to a hollow metal tube which opens underneath the spoon. The hollow tube passes through a series of fittings to fasten it to the appropriate aperture for producing air bubbles of different sizes.

The experimental set-up consists also of a high resolution CCD video camera mounted on a lifting device capable of moving up and down at different speeds. The lifting device is powered by an adjustable speed motor connected to a pulley system which allowed the camera to move up with the rising bubble. The video output from the camera was then fed to a computer. The video was viewed using Windows Movie Maker and still frames were viewed using DV Studio software. The software was used for measuring the volume, area, perimeter, diameter, trajectory and the velocity with the vertical axis of symmetry. The data obtained from the software was used to calculate other parameters, such as, Reynolds number and the drag coefficient of various bubbles.

Fluids. Water, polymer solutions of 0.025% and 0.045% by weight of polyacrylamide were used in this research. The polyacrylamide solutions were prepared adding polyacrylamide and water in a bucket and stirring over many hours to ensure homgeneous mixing.

Fluid characterisation. The rheological characterizations of massecuite and polyacrylamide solutions (0.025% and 0.045%) were carried out using the ARES rheometer. Firstly, the rheological properties of massecuite (40% massecuite) at 65°C were characterised and are presented in Figure 1. The rheological tests were carried out for a maximum shear rate of 30 sec^{-1} and the reults show a Power-law behaviour which is described by.

$$\eta = K(\dot{\gamma})^{n-1} \qquad (1)$$

Here, η is the viscosity, K is the fluid consistency; n is the power index and $\dot{\gamma}$ is the shear rate.

The replacement solution for massecuite was selected after various percentage combinations of polyacrylamide and water were prepared and tested. The polyacrylamide solution of 0.045% by weight was seen to yield the rheological properties similar to that of massecuite. In particular, this solution showed the same viscosity at lower shear rate as that of massecuite solution. However, the density and elasticity of this solution were different from that of the massecuite mixture since it was difficult to match those values. The density of this polyacrylamide solution was 998.5 kg/m^3. It is noted that further work are in progress to develop a massecuite-equivalent transparent solution and study the influence of these parameters on the bubbles.

Bubble injection operation. The interchangeable bubble insertion mechanism which was screwed in the aperture at the bottom of the tube was used for the bubble generation. Bubble sizes produced were approximately 0.1 ml and 0.2 ml in the 125 mm polycarbonate tube and 2 ml, 5 ml, 10 ml 15 ml and 20 ml in the 400 mm diameter acrylic tube.

Bubble velocity and trajectory. Bubble velocity was determined from the video footage of each bubble. Once the bubble was released, the video camera moved up with the bubble recording the images as it rose through various markers which were positioned at an interval of 100 mm from the bottom to a height of 1 meter. Velocity was measured for a 100 mm distance and was averaged for the entire 1 meter travel. Bubble trajectory was determined from the still frames obtained from the video image.

The drag coefficient of a bubble can be calculated by

$$C_D = \frac{2F_D}{\rho_{liquid} V^2 A} \qquad (2)$$

Where F_D is the drag force acting on the bubble, ρ_{liquid} is the density of the liquid, V is the velocity of the bubble and A is the area of the bubble.

Results and discussion

Velocity. Velocities of water and two polymeric solutions are presented respectively in Figure 2, Figure 3 and Figure 4. In those figures, the data are indicated by, for water: S1=0.1 ml bubble; S2=0.2 ml bubble; S3=0.2 ml bubble with additional water head and for polymeric solution: S4=0.1 ml bubble and S5=0.2 ml bubble. As seen, the rise velocities over the distance of 1 m fluctuated (from a mean value) at various depths. However, the mean of these velocities give a fairly constant value over the entire one meter rise. For example, S4 has an average velocity of 0.241 ms^{-1} while S5 has an average velocity of 0.232 ms^{-1}.

For bubble group S5, there is a downward spike in the average velocity between 100-200mm that also has a low standard deviation. Also, before this point there exists a large spike. This spike is due from the initial acceleration of the bubble as it tries to reach an equilibrium state and terminal velocity. On comparing the velocity results of the polymeric solution with that of water, the fluctuations are more pronounced for smaller bubbles in water than those in polymer. For polymeric solutions, the bubbles appear better behaved and the graphs appear a lot smoother.

Figure 5 shows the mean velocity of 0.045% solution for each bubble size. As seen, the velocity is increasing with the increase in bubble size. The buoyancy force of bigger bubble is seen to give a higher velocity overcoming the friction.

Trajectory. When the bubble is released, the general trend is for it to remain close to the release centre and as it rises through the liquid it spreads out.

For bubbles in water, trajectory becomes more disperse. It is seen that under the same conditions, small bubbles (S1) had a lower spread. For an increased pressure on the top of the liquid column (water column was increased from 155 mm to 355 mm), the spread for the same size (S3) bubble is reduced.

For polymer solutions, the results show an opposite trend of those in water where the smaller bubbles would deviate more than the larger bubbles. The 0.1 ml bubbles were very well behaved, and hardly differed from their alignment with the injection point. For the larger 0.2 ml bubbles, the spread was much broader, but still not as broad as that for bubble in water. For the 0.2 ml bubbles, they exhibited a large initial increase in standard deviation between 0 mm and 200 mm rise. This is due to the bubble reaching its terminal velocity and equilibrium state and shape. This trend is attributed to the properties of the polymer, primarily the viscosity and elasticity.

Analysis of drag coefficient. For the analysis of drag using Eq. 2, the surface area of the bubble was calculated from the equivalent diameter of the bubble. This effectively reduced the volume of the bubble, regardless of the shape, into a single value that describes a bubble of same volume but spherical shape. Since the surface area of a spherical bubble is $4\pi D^2$ this is substituted in for *A*.

F_D is the drag force acting upon the bubble. It has two components. The first component is due to the pressure of the fluid on the bubble. Surface tension and effects of fluid elasticity upon the bubble cause the second component.
For a Newtonian liquid, the drag force is given by $F_D = 6\pi\mu_{fluid} RV$ where *R* is the radius of a sphere and given by $D^3 = (R/2)^3 = hw^3$ where *h* is defined as the height of the bubble and *w* is the bubble width. This does make the assumption that the bubble is axisymmetric and either spherical or elliptical in form.

The equation for drag force of a non-Newtonian liquid differs slightly from that of a Newtonian liquid. However, the non-Newtonian effects (in particular the decrease in viscosity as object speed increase) are viewed as not dominant for the polymer solution used, and the above formula is considered sufficient in this example.

The correlation between the Reynolds number and the drag coefficient were calculated. The empirical relations are For S1 data, $C_D=43.582Re^{1.114}$; for S2 data, $C_D=151.98Re^{1.274}$, for polymer S4 data, $C_D=96.717Re^{1.2667}$ and for S5 data, $C_D=62.212Re^{1.191}$. These values appear to differ from the theoretical by a constant factor.

Bubble volume. In this investigations various sizes of bubble were used for both water and polymeric solutions. In particular, for 0.045% solution, the bigger sizes bubbles of 2 ml, 10 ml, 15 ml and 20 ml were used. Figure 6 shows photographs of different shape and size of the bubbles as they rise through 0.045% solution in the 400 mm acrylic tube.

Summary

The velocity showed how the speed differs as the bubble rises. The trajectory also illustrated the trends of the bubbles. An interesting outcome was the opposite trend of the bubble in polymeric solution, that is, unlike in water, the spread of the trajectory increased with the increase of bubble size. This is most likely due to elasticity and relatively higher viscosity of polymeric solutions. The drag coefficient produced acceptable results although the results are seen to differ from the theoretical approximate by a constant. The velocity, trajectory, drag coefficient and other parameters monitored and calculated from this new experimental setup provide important results in furthering the understanding of bubble rise through non-Newtonian liquids.

References

[1] Stephens, D.W. (2001), Studies on modelling circulation in sugar vacuum pans, Ph.D. Thesis, James Cook University, Townsville.

[2] Rouillard, E.E.A. (1985), Massecuite boiling, Proc. S. Afr. Sugar Technol. Ass., 59:43-47.

[3] Bröder, D. and Sommerfeld, M. (2002), An advanced LIF-PLV system for analyzing the hydrodynamics in a laboratory bubble column at higher void fractions, Experiments in Fluids, Journals Springer Verlag, p23.

[4] Jiang, P., Luo, X. and Lin, J. (1995), Flow visualization of a high pressure and high temperature bubble column, Chemical Engineering Research and Design (The Transactions of the Institute of Chemical Engineers, UK), 73, part A, pp. 269-274.

[5] Behzadi, A., Issa, R.I. and Rusche, H. (2004), Modelling of dispersed bubble and droplet flow at high phase fractions, Chemical Engineering Science, 59:759–770.

[6] Chhabra, R.P. (1993), Bubbles, drops and particles in non-Newtonian fluids, CRC Press, Boca Raton, Fla.

[7] Samir, K (1994), Mechanism of heat transfer in bubble columns and three-phase fluidization systems with viscous liquids, AIChE J., 40 (5) 754-755

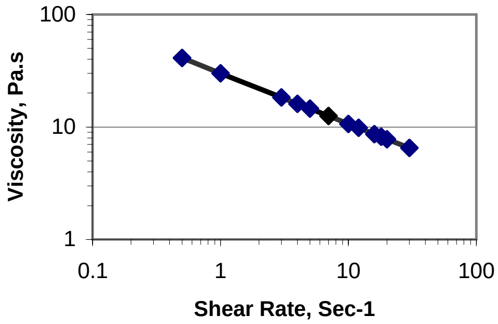

Fig 1. Viscosity vs shear rate for 40% massecuite

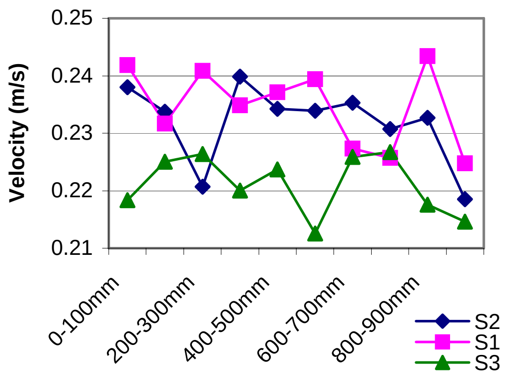

Fig .2. Velocity vs bubble rise distance in water

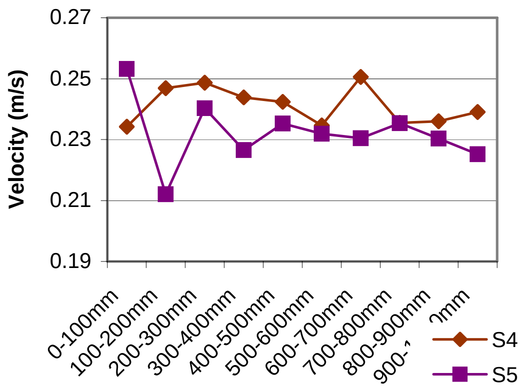

Fig 3. Velocity vs bubble rise distance in 0.025% solution

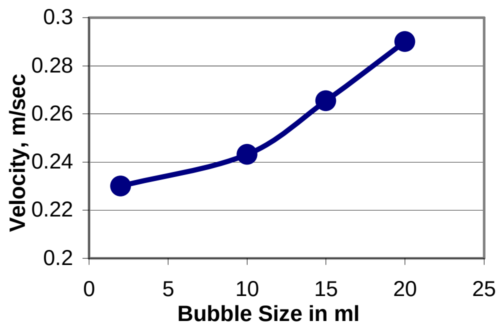

Fig 4. Velocity vs bubble size in 0.045% solution

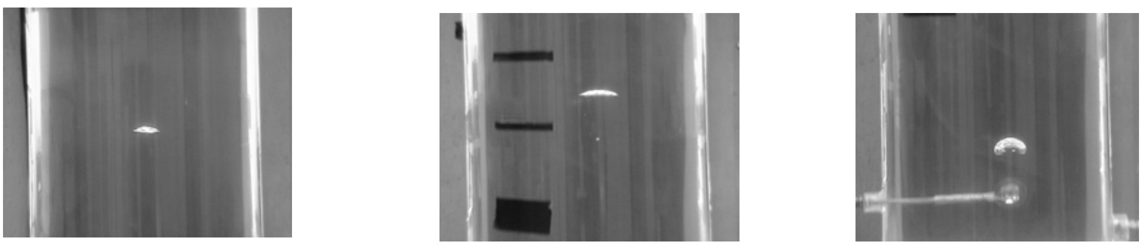

Fig 5. Different sizes of bubble rise in 0.045% solution